Supplementary Information

1. Experimental section

Materials and methods

NMR spectra were recorded on a JEOL EX 400 spectrometer (^{1}H operating frequency 400 MHz) at 298 K and data were treated by Jeol Delta Software. ^{1}H and ^{13}C chemical shifts are reported relative to TMS ($\delta = 0$) and referenced against solvent residual peaks. The following abbreviations are used: s, singlet; d, doublet; t, triplet; m, multiplet; td, triplet of doublets; ddd, doublet of doublets of doublets. The samples for microanalyses were dried in vacuum to constant weight (20°C, ca. 0.1 Torr). Elemental analyses (C, H, N) were performed in-house with a Fisons Instruments 1108 CHNS-O Elemental Analyzer.

Syntheses

Reagents were purchased from Aldrich and employed as received. Solvents were purged for 10 minutes with argon before use. All the manipulations of the Mn complexes were performed in the dark.

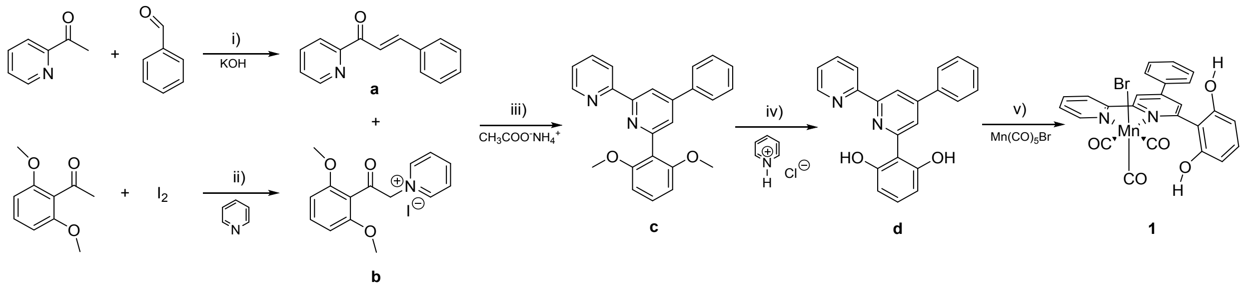

Scheme S1. Synthetic route for the synthesis of the ligand dhbpy (4-phenyl 6-(1,3-dihydroxy-benzen-2-yl) 2,2'-bipyridine), **d**, and **1**; i) water, 4°C, 24 h; ii) pyridine, reflux, 3 h; iii) CH_3OH, reflux, 6 h; iv) reflux, 3 h; v) diethyl ether, reflux, 4h.

Synthesis of (E)-3-phenyl-1-(pyridin-2-yl)prop-2-en-1-one (a). An emulsion of benzaldehyde (19 mmol) in cold distilled water (100 ml) was prepared in a flask and then an equimolar amount of 1-(pyridin-2-yl)ethanone was added under vigorous stirring. A solution of 10% KOH in water (10ml) was then added dropwise and the mixture became pale yellow. The emulsion was stirred for 24 hours at 4°C and the yellow product was filtered and washed with water and methanol (yield 98%). [1]

^{1}H-NMR [400 MHz, $(CD_3)_2CO$]: δ/ppm = 8.79 (d, J = 4.7 Hz, 1H), 8.38 (d, J = 16.1 Hz, 1H), 8.15 (d, J = 7.7 Hz, 1H), 8.04 (td, ^{1}J = 7.6 Hz, ^{2}J = 1.5 Hz, 1H), 7.89 (d, J = 16.1 Hz, 1H), 7.82 (m, 2H), 7.66 (ddd, ^{1}J = 7.6 Hz, ^{2}J = 5.0 Hz, ^{3}J = 1.5 Hz, 1H), 7.49 (m, 3H).

Synthesis of 1-(2-(2,6-dimethoxyphenyl)-2-oxoethyl)pyridinium iodide (b). 20 mmol of 1-(2,6-dimethoxyphenyl)ethanone and 24 mmol of iodine were refluxed for 3 hours in 50 ml of pyridine. The reaction mixture was cooled to 0° C and the yellow product was precipitated, filtered and washed with cold pyridine (yield 88%). [2]

^{1}H-NMR [400 MHz, $(CD_3)_2CO$]: δ/ppm = 9.19 (d, J = 6.6 Hz, 2H), 8.88 (t, J = 7.6 Hz, 1H), 8.40 (t, J = 6.8 Hz, 2H), 7.50 (t, J = 8.5 Hz, 1H), 6.81 (d, J = 8.5 Hz, 2H), 6.30 (s, 2H), 3.92 (s, 6H).

Synthesis of 6-(2,6-dimethoxyphenyl)-4-phenyl-2,2'-bipyridine (c). A suspension of 11 mmol of **b**, 11 mmol of **a** and 0.110 mol of ammonium acetate was refluxed in methanol (30 ml) for 6 hours. The mixture was then cooled to room temperature and the yellow product was filtered and washed with cold methanol (yield 83%). [3]

^{1}H-NMR [400 MHz, $(CD_3)_2CO$]: δ/ppm = 8.71 (m, 2H), 8.47 (d, J = 8.2 Hz, 1H), 7.89 (m, 3H), 7.57 (m, 3H), 7.50 (t, J = 8.5 Hz, 1H), 7.40 (m, 2H), 6.81 (d, J = 8.2 Hz, 2H), 3.74 (s, 6H).

^{13}C-NMR [100 MHz, $(CD_3)_2CO$]: δ/ppm = 159.31, 157.27, 157.07, 156.08, 150.07, 149.42, 139.50, 137.95, 137.65, 130.63, 130.11, 129.87, 127.90, 124.80, 124.67, 121.83, 117.11, 105.41, 56.38.

Synthesis of 2-(4-phenyl-2,2'-bipyridin-6-yl)benzene-1,3-diol (d). In a three-necked flask pyridinium chloride was prepared by heating a mixture of concentrated HCl (17.6 ml) and pyridine (16 ml) for 2 hours at 195° C under a flow of Ar. Then, **c** (0.3 mmol) was added and the reaction mixture was heated at 195° C under Ar for 3 hours. Once cooled to room temperature, the solid was dissolved in 20 ml of H_2O and neutralized with an aqueous solution of KOH. The solid product was then filtered and washed with H_2O and CH_2Cl_2 (Yield 71%). [4]

^{1}H-NMR [400 MHz, $(CD_3)_2SO$]: δ/ppm = 8.79 (m, 2H), 8.52 (s, 1H), 8.24 (d, J = 8.2 Hz, 1H), 8.06 (t, J = 7.6 Hz, 1H), 7.88 (d, J = 7.3 Hz, 2H), 7.60 (m, 2H), 7.55 (m, 2H), 7.12 (t, J = 8.2 Hz, 1H), 6.49 (d, J = 7.9 Hz, 2H).

^{13}C-NMR [100 MHz, $(CD_3)_2SO$]: δ/ppm = 158.64, 156.13, 154.02, 152.84, 149.87, 149.79, 137.81, 130.88, 129.56, 129.43, 127.08, 124.67, 123.00, 120.60, 116.37, 108.80, 107.61.

IR (ATR): 3100-3300 (br.), 3057, 1606 cm^{-1}.

Synthesis of [Mn(dhbpy)(CO)$_3$Br] (1). $Mn(CO)_5Br$ (1 eq) and **d** (1.01 eq) were refluxed for 4 hours in diethyl ether under stirring. The reaction mixture was then cooled to room temperature and the yellow product was filtered and washed once with diethyl ether (yield 71 %).

^{1}H-NMR [400 MHz, $(CD_3)_2CO$]: δ/ppm = 9.34 (d, J = 4.9 Hz, 1H), 8.85 (m, 2H), 8.76 (s, 1H), 8.25 (t, J = 5.3 Hz, 1H), 8.06 (d, J = 5.8 Hz, 2H), 7.88 (s, 1H), 7.74 (t, J = 5.3 Hz, 1H), 7.58 (m, 3H), 7.27 (s, 1H), 7.23 (t, J = 8.2 Hz, 1H), 6.67 (d, J = 7.9 Hz, 1H), 6.60 (d, J = 7.9 Hz, 1H).

^{13}C-NMR [100 MHz, $(CD_3)_2CO$]: δ/ppm = 161.31, 158.27, 157.46, 156.64, 156.57, 154.07, 151.27, 139.69, 136.84, 132.36, 131.17, 130.25, 128.41, 127.64, 127.14, 124.49, 120.17, 110.84, 108.78.

IR (ATR): 3320, 2018, 1931,1899 cm^{-1}. Anal. Calcd. (%) for $C_{25}H_{16}BrN_2O_5Mn$: C 53.69, H 2.88, N 5.01. Found: C 53.76, H 2.81, N 4.98.

Synthesis of [Mn(dmobpy)(CO)$_3$Br] (2). $MnCO_5Br$ (1 eq) and **c** (1.01 eq) were refluxed for 4 hours in diethyl ether under stirring. The reaction mixture was then cooled to room temperature and the yellow product was filtered and washed once with diethyl ether (yield 78 %).

^{1}H-NMR [400 MHz, $(CD_3)_2CO$]: δ/ppm = 9.30 (d, J = 5.4 Hz, 1H), 8.81 (m, 2H), 8.22 (t, J = 7.9 Hz, 1H), 8.03 (d, J = 7.0 Hz, 2H), 7.78 (s, 1H), 7.70 (t, J = 6.8 Hz, 1H), 7.58 (m, 3H), 7.50 (t, J = 8.5 Hz 1H), 6.81 (m, 2H), 3.79 (s, 3H), 3.73 (s, 3H).

^{13}C-NMR [100 MHz, $(CD_3)_2CO$]: δ/ppm = 161.24, 159.74, 158.62, 158.45, 157.58, 153.92, 150.60, 139.45, 136.95, 132.76, 131.05, 130.23, 128.35, 127.13, 126.77, 124.31, 121.29, 119.71, 106.08, 104.24, 56.63, 55.78.

IR (ATR): 2017, 1931, 1900 cm^{-1}. Anal. Calcd. (%) for $C_{27}H_{20}BrN_2O_5Mn$: C 55.22, H 3.43, N 4.77. Found: C 55.04, H 3.39, N 4.84.

Cyclic Voltammetry (CV)

All the solvents used for electrochemical experiments were freshly distilled. Cyclic voltammetry experiments were performed with a Metrohm Autolab 302N potentiostat. 1 mM solutions of compounds **1** and **2** in CH_3CN were used, with tetrabutylammonium hexafluorophosphate ($TBAPF_6$) as supporting electrolyte (0.1 M). A single-compartment cell was employed, with a glassy carbon (GC) working electrode (Ø = 1 mm), a Pt counter electrode and an aqueous SCE as reference electrode. All the CVs were performed in the dark. In our conditions the redox couple Fc/Fc^+ in CH_3CN has been observed at $E_{1/2} = 0.39$ V ($\Delta E_p = 62$ mV). The Ar- and CO_2-saturated conditions were achieved by purging gases for 5 minutes before each potential sweep.

Controlled-Potential Electrolysis (CPE)

The experiments were carried out using a Metrohm Autolab 302N potentiostat. A double compartment H-type cell was employed, a Pt wire as counter electrode in a bridge separated from the cathodic compartment by a glass frit. A glassy carbon working electrode (A = 12.35 cm^2) and an aqueous SCE reference electrode were also used. CPE experiments were performed in acetonitrile with 0.1 M $TBAPF_6$ as supporting electrolyte, and 1.0 mM of **1** at –1.5 V and at –1.8 V *vs.* SCE. A constant flow of CO_2 (20 ml/min) was maintained during the CPE measurements.

Detection of the CO_2 reduction products

Gaseous products. A Smart Trak 100 (Sierra) flow controller C100L was used during the electrochemical experiments. The gas sample was analyzed by means of an Agilent 490 Micro GC gas chromatograph equipped with a Molsieve 5 Å column and a CP-PoraPLOT U column. For the CO and H_2 quantification a thermal conductivity detector was used and the Molsieve 5 Å column was kept at a temperature of 90° C and at a pressure of 200 kPa. The carrier gas was argon. For the functioning and the calibration of the GC apparatus, Ar, He, N_2, O_2, CO_2 and CO were obtained from Sapio, whereas H_2 was produced with a Claind HyGen hydrogen generator. The limits of detection for CO and H_2 were 20 ppmv and 0.5 ppmv respectively.

Formic acid. Formic acid production was evaluated with ion chromatography, employing a Dionex DX 500 instrument equipped with a Dionex IonPac® AS9-HC column (200 mm × 4 mm i.d.), GP40 pump (Dionex), an electrochemical detector ED40 (Dionex) and an Anion Self-Regenerating Suppressor-Ultra (ARSR®-ULTRA, 4-mm, Dionex). Elution was performed in isocratic conditions with an aqueous solution of K_2CO_3 9.0 10^{-3} M at 0.90 mL min^{-1} flow rate. In those conditions we observed a retention time of 5.45 min for the formate anion (Fig. S2). For the analysis the $TBAPF_6$ matrix has to be removed, therefore, after basification with ammonia, we dried the CPE solution in vacuum at room temperature. At this point we added 10.0 mL of NaOH 0.01 M, filtered the sample and, to remove the remaining $TBAPF_6$ and **1**, we injected 1.00 mL of the sample in a disposable SPE column (containing BAKERBOND spe™ Quaternary Amine (N^+) and Carlo Erba Amberlite® CG-120, previously conditioned with HCl 0.01 M) and eluted with 9.00 mL of HCl 0.01M. The resulting solutions were brought to pH 12 and analyzed by means of ion chromatography.

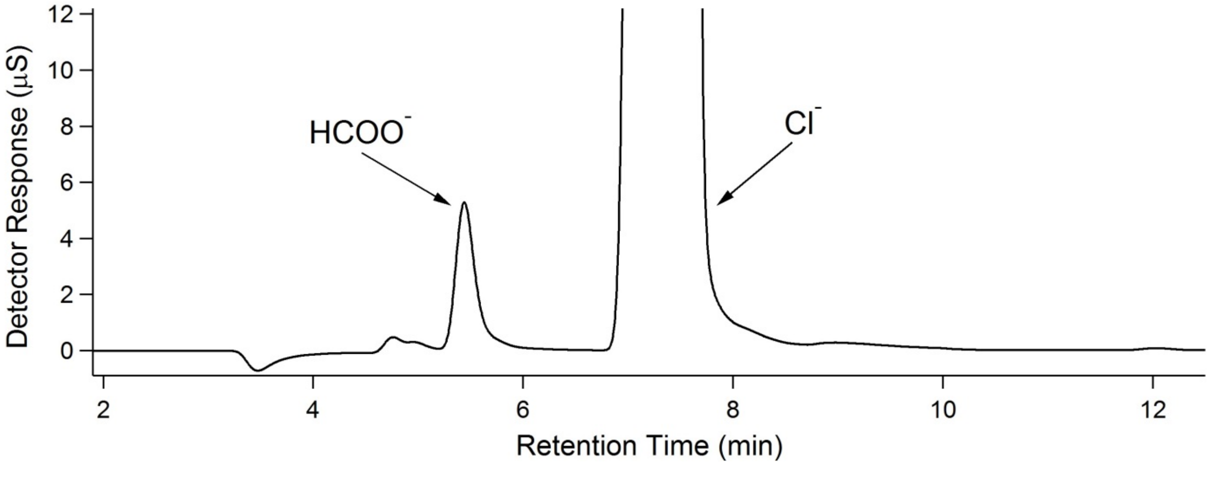

Fig. S2 – Chromatogram related to the CPE of [Mn(dhbpy)$(CO)_3$Br] (**1**) at –1.8 V vs SCE after four hours of experiment. The presence of chloride is due to the sample treatment, necessary to remove the $TBAPF_6$ matrix.

2. X-ray Crystallographic Analysis

The X-ray data of complex **1** crystal have been collected on a Gemini R Ultra diffractometer with a Cu Kα (= 1.54184 Å) at room temperature.[5] The crystal data and refinement results are collected in Table S1 and S2. CrysAlisPro [6] was the software used for data collection and integration, SHELXTL [7] was employed for solving structures and for conventional refinement. Molecular graphics was made by using the CrystalMaker program.

Table S1. Crystallographic Data for [Mn(dhbpy)$(CO)_3$Br] (**1**).

	[Mn(dhbpy)$(CO)_3$Br] (1)
Empirical formula	$Mn_1\ Br_1\ C_{29}\ N_2\ O_6\ H_{26}$
Formula weight	633.36
Temperature (K)	293(2)
Wavelength (Å)	1.54184
Space group	P-1
a (Å)	11.3412(5)
b (Å)	11.5546(5)
c (Å)	12.4448(6)
α (deg)	71.684(4)
β (deg)	69.151(4)
γ (deg)	79.227(4)
Volume (Å^3)	1441.62(11)
Z	2
Density calculated (g cm^{-3})	1.459
μ (mm^{-1})	1.851
R	0.0413
R_w	0.1052

Table S2. Experimental bond lengths (Å) and angles (°) for [Mn(dhbpy)(CO)$_3$Br] (**1**).

Mn(1)-C(25)	1.788(6)
Mn(1)-C(23)	1.795(6)
Mn(1)-C(24)	1.818(6)
Mn(1)-N(1)	2.042(4)
Mn(1)-N(2)	2.087(4)
Mn(1)-Br(1)	2.5483(9)
N(1)-C(5)	1.343(6)
N(1)-C(1)	1.348(6)
C(1)-C(2)	1.374(8)
C(2)-C(3)	1.360(8)
C(3)-C(4)	1.385(7)
C(4)-C(5)	1.395(7)
C(5)-C(6)	1.473(6)
N(2)-C(10)	1.350(6)
N(2)-C(6)	1.360(5)
C(6)-C(7)	1.375(6)
C(7)-C(8)	1.393(6)
C(8)-C(9)	1.376(6)
C(8)-C(11)	1.481(7)
C(9)-C(10)	1.390(6)
C(10)-C(17)	1.488(6)
C(11)-C(12)	1.380(8)
C(11)-C(16)	1.384(8)
C(12)-C(13)	1.385(9)
C(13)-C(14)	1.360(11)
C(14)-C(15)	1.352(11)
C(15)-C(16)	1.390(9)
C(17)-C(22)	1.382(6)
C(17)-C(18)	1.392(7)
C(18)-O(2)	1.361(6)
C(18)-C(19)	1.381(7)
C(19)-C(20)	1.368(8)
C(20)-C(21)	1.374(8)
C(21)-C(22)	1.384(7)
C(22)-O(1)	1.363(6)
C(23)-O(3)	1.128(6)
C(24)-O(4)	1.146(6)
C(25)-O(5)	1.143(6)
C(26)-C(27)	1.261(17)
C(27)-O(6)	1.394(12)
C(28A)-C(29A)	1.365(18)
C(28A)-O(6)	1.410(17)
C(28B)-C(29B)	1.432(18)
C(28B)-O(6)	1.508(17)
C(25)-Mn(1)-C(23)	90.2(2)
C(25)-Mn(1)-C(24)	86.1(3)
C(23)-Mn(1)-C(24)	92.4(2)
C(25)-Mn(1)-N(1)	94.1(2)
C(23)-Mn(1)-N(1)	91.4(2)

C(24)-Mn(1)-N(1)	176.2(2)
C(25)-Mn(1)-N(2)	169.7(2)
C(23)-Mn(1)-N(2)	97.15(19)
C(24)-Mn(1)-N(2)	100.78(19)
N(1)-Mn(1)-N(2)	78.57(15)
C(25)-Mn(1)-Br(1)	87.42(18)
C(23)-Mn(1)-Br(1)	177.60(17)
C(24)-Mn(1)-Br(1)	87.58(17)
N(1)-Mn(1)-Br(1)	88.64(11)
N(2)-Mn(1)-Br(1)	85.20(10)
C(5)-N(1)-C(1)	118.4(4)
C(5)-N(1)-Mn(1)	115.7(3)
C(1)-N(1)-Mn(1)	125.9(4)
N(1)-C(1)-C(2)	122.3(5)
C(3)-C(2)-C(1)	119.7(5)
C(2)-C(3)-C(4)	119.0(5)
C(3)-C(4)-C(5)	119.0(5)
N(1)-C(5)-C(4)	121.5(4)
N(1)-C(5)-C(6)	115.5(4)
C(4)-C(5)-C(6)	122.9(5)
C(10)-N(2)-C(6)	117.3(4)
C(10)-N(2)-Mn(1)	128.5(3)
C(6)-N(2)-Mn(1)	113.3(3)
N(2)-C(6)-C(7)	122.8(4)
N(2)-C(6)-C(5)	114.1(4)
C(7)-C(6)-C(5)	123.0(4)
C(6)-C(7)-C(8)	120.7(4)
C(9)-C(8)-C(7)	115.6(4)
C(9)-C(8)-C(11)	122.0(4)
C(7)-C(8)-C(11)	122.4(4)
C(8)-C(9)-C(10)	122.4(4)
N(2)-C(10)-C(9)	121.1(4)
N(2)-C(10)-C(17)	120.9(4)
C(9)-C(10)-C(17)	118.0(4)
C(12)-C(11)-C(16)	118.5(5)
C(12)-C(11)-C(8)	121.3(5)
C(16)-C(11)-C(8)	120.1(5)
C(11)-C(12)-C(13)	120.2(7)
C(14)-C(13)-C(12)	120.7(7)
C(15)-C(14)-C(13)	119.8(7)
C(14)-C(15)-C(16)	120.8(7)
C(11)-C(16)-C(15)	120.0(7)
C(22)-C(17)-C(18)	119.0(4)
C(22)-C(17)-C(10)	120.6(4)
C(18)-C(17)-C(10)	119.9(4)
O(2)-C(18)-C(19)	123.2(5)
O(2)-C(18)-C(17)	116.5(4)
C(19)-C(18)-C(17)	120.3(5)
C(20)-C(19)-C(18)	119.3(5)
C(19)-C(20)-C(21)	121.8(5)
C(20)-C(21)-C(22)	118.8(5)

O(1)-C(22)-C(17)	116.8(4)
O(1)-C(22)-C(21)	122.4(4)
C(17)-C(22)-C(21)	120.8(5)
O(3)-C(23)-Mn(1)	175.1(5)
O(4)-C(24)-Mn(1)	173.4(5)
O(5)-C(25)-Mn(1)	179.2(6)
C(26)-C(27)-O(6)	114.6(13)
C(29A)-C(28A)-O(6)	112(2)
C(29B)-C(28B)-O(6)	108(2)
C(28A)-O(6)-C(27)	110.0(15)
C(28A)-O(6)-C(28B)	38.2(12)
C(27)-O(6)-C(28B)	126.4(15)

3. Electrochemical details

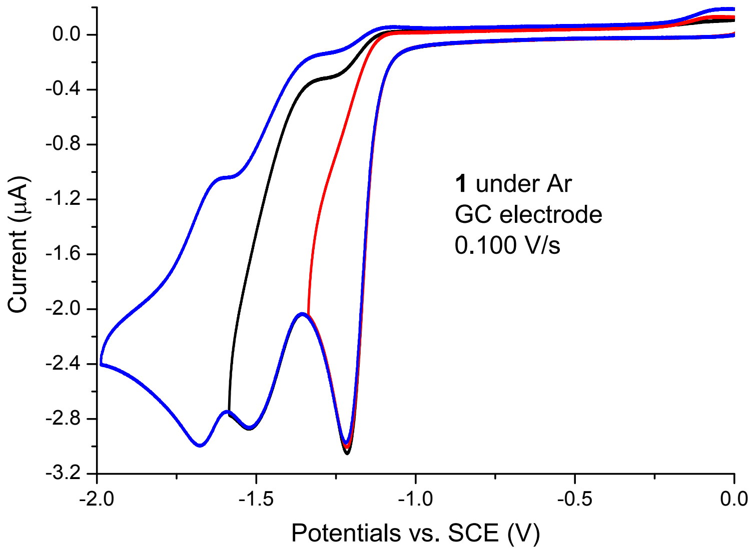

Fig. S3 CVs of 1 mM acetonitrile solution of **1** at 100 mV s^{-1} on a glassy carbon electrode in $TBAPF_6$ 0.1 M under Ar at different switching potentials.

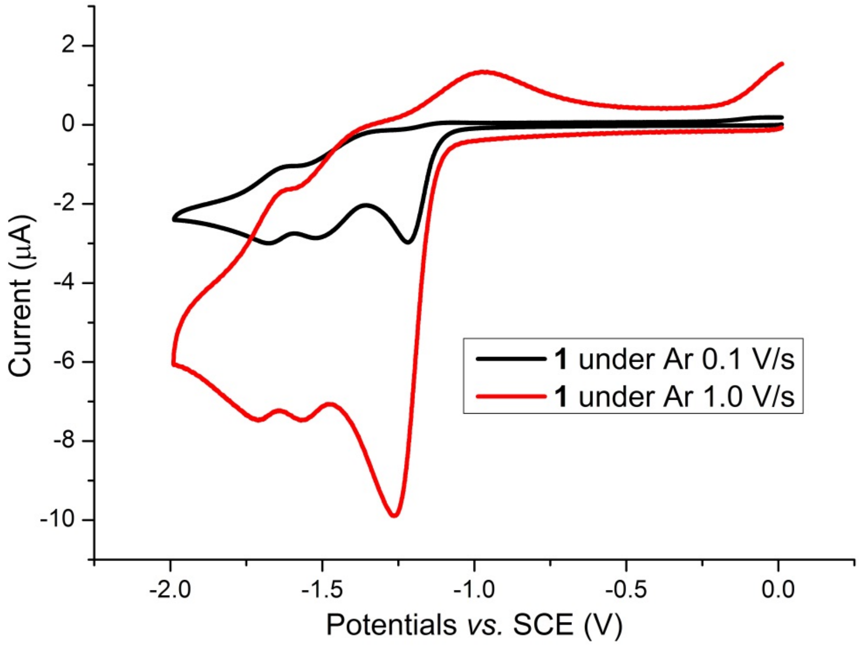

Fig. S4 CVs of 1 mM acetonitrile solution of **1** at 100 mV s^{-1} and 1.0 V s^{-1} on a glassy carbon electrode in $TBAPF_6$ 0.1 M under Ar.

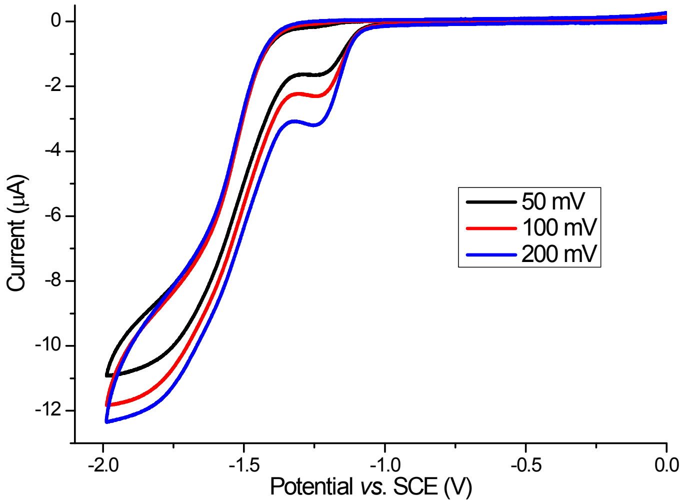

Fig. S5 CVs of 1 mM acetonitrile solution of **1** at 50 mV s^{-1} (black line), 100 mV s^{-1} (red line) and 200 mV s^{-1} (blue line) on a glassy carbon electrode in $TBAPF_6$ 0.1 M under CO_2-saturated atmosphere.

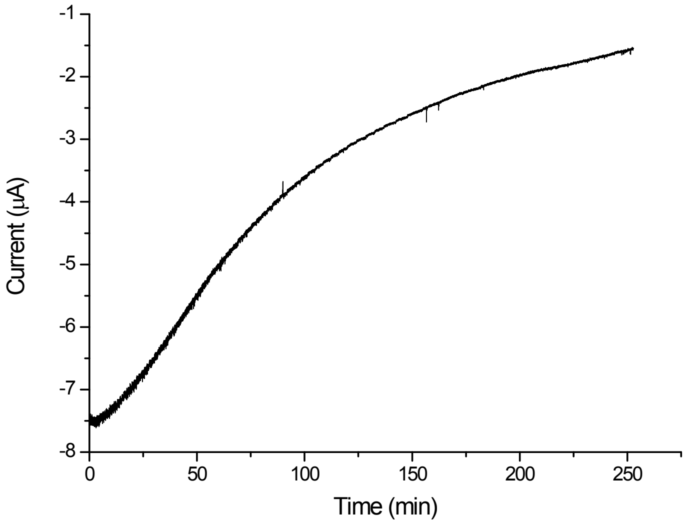

Fig. S6 Chronoamperometry during bulk electrolysis of a 1 mM acetonitrile solution of [Mn-(dhbpy)(CO)$_3$Br] (**1**) under CO$_2$ at –1.8 V *vs.* SCE over four hours.

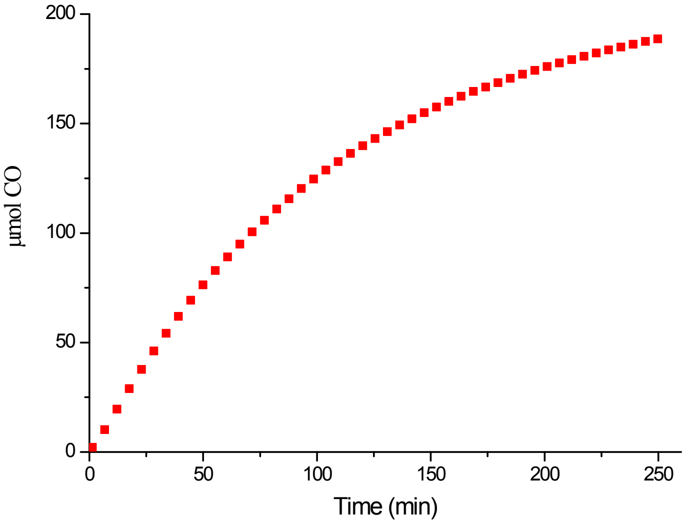

Fig. S7 Overall CO production during four hours of electrolysis performed at –1.8 V *vs.* SCE of a 1 mM acetonitrile solution of [Mn(dhbpy)(CO)$_3$Br] (**1**). Sampling of gaseous CO was automatically made every five minutes of analysis by gas chromatography.

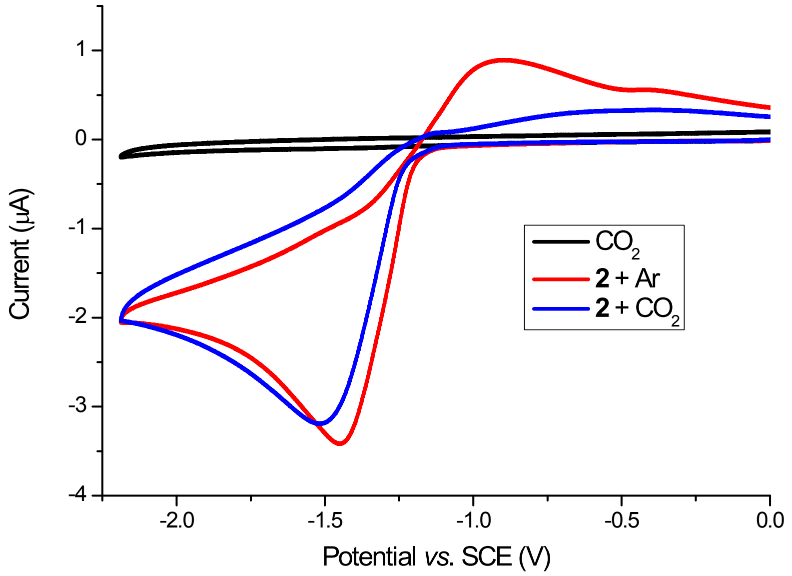

Fig. S8. CVs of a 1 mM acetonitrile solution of [Mn(dmobpy)(CO)$_3$Br], (**2**), at 100 mV s^{-1} (GC working electrode, TBAPF$_6$ 0.1 M) under Ar (red) or CO$_2$ (blue). The black CV is the CO$_2$ saturated background.

4. Calculation of TOF values from bulk electrolysis

The kinetic parameters reported for the complex **1** were obtained from controlled-potential electrolysis, by using the theoretical treatment developed by Saveant and Costentin. [8] Accordingly to some recent applications of this model to similar catalytic systems [9], a useful expression for Turnover Frequency (TOF), eq. (3), can be derived from the following eq. (1-2):

$$\frac{i}{FA} = \frac{\sqrt{k_{cat} D}\, C_{cat}}{1 + exp\text{â}\square\text{¡}\left[\frac{F}{RT}\left(E_{applied} - E^{\,0}_{cat}\right)\right]} \qquad (1)$$

$$k_{cat} = 2kC^0_A = \frac{i^2\left\{1 + \exp\left[\frac{F}{RT}\left(E_{applied} - E^{\,0}_{cat}\right)\right]\right\}^2}{F^2 A^2 C^{\,2}_{cat} D} \qquad (2)$$

$$TOF = \frac{kC^0_A}{1 + \exp\left[\frac{F}{RT}\left(E_{applied} - E^{\,0}_{cat}\right)\right]}\text{â\%oˆ}kC^0_A \quad for\ E_{applied}\text{â\%oª}E^{\,0}_{cat} \qquad (3)$$

where kC_A^0 is the pseudo-first order constant, k_{cat} is the overall rate constant of the catalytic process, C_A^0 is the initial concentration of substrate, C_{cat} is the catalyst concentration in the bulk, whereas the other parameters are straightforward. It is noteworthy that in eq. (1-2), i describes the steady-state current achieved during first 10 minutes of electrolysis, but, because of lack of selectivity occurred for **1**, this value should be multiplied for the Faradaic efficiency for CO production (η_{CO}), in order to accurately calculate the k_{CO} and TOF_{CO} parameters. Furthermore, in principle, the knowledge of the standard potential of the catalyst redox couple, E_{cat}^0, is mandatory for the calculation of TOF, as suggested by eq. (3). However, this relationship can be reasonably simplified, by performing bulk electrolysis at a potential value characterized by limiting current, so that the operating potential value, $E_{applied}$, is significantly more cathodic than E_{cat}^0, and the exponential term in eq. (2) becomes negligible. It should be noted also that the numeric value used here for the diffusion coefficient D of the catalytically active species was assumed equal to that already reported for other structurally similar Mn(I) catalysts. [9] To summarize, the following data were employed for calculations:

$i = 0.007336$ A
$\eta_{CO} = 0.7018$
$i_{CO} = 0.005149$ A
$F/RT = 38.94\ \mathrm{V}^{-1}$
$A = 12.35\ \mathrm{cm}^2$
$D = 1.1\times10^{-5}\ \mathrm{cm}^2\ \mathrm{s}^{-1}$ [From Ref. 9]
$C_{cat} = 7.703\times10^{-7}\ \mathrm{mol\ cm}^{-3}$
$E_{applied} = -1.8$ V *vs* SCE
$C_A^0 = 0.28$ M [From Ref. 10]
$\boldsymbol{k_{CO} = 5.11\ \mathrm{M}^{-1}\ \mathrm{s}^{-1}}$
$\boldsymbol{TOF_{CO} = 1.43\ \mathrm{s}^{-1}}$

5. Computational details

Gaussian 09 rev. C.01 was employed for all calculations. Geometry optimization was performed with the B3LYP functional including the conductor-like polarizable continuum model method (CPCM) with acetonitrile as solvent. The LanL2DZ and 6-31G(d,p) basis sets were used for Mn and for the other atoms, respectively. Unrestricted approach was adopted for calculations on systems with odd number of electrons. The nature of all stationary points was confirmed by performing a normal-mode analysis..

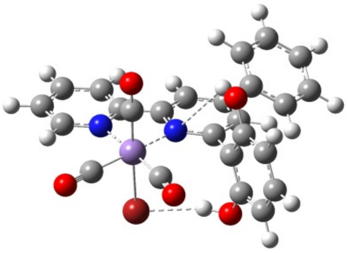

Optimized geometry of **1**, [Mn(dhbpy)(CO)$_3$Br]:

Br	-1.88520200	-0.27703400	2.28111200
Mn	-2.05287200	-0.31716100	-0.32766100
N	0.05539700	-0.17313500	-0.27639700
C	-0.18651800	-2.56856800	-0.25198900
O	0.33642100	2.38512500	-2.68316600
H	0.67504800	1.48890800	-2.54642100
C	0.68653200	-1.37811900	-0.22143600
C	0.82616600	0.94207400	-0.21649800
C	-0.03135900	3.00950800	0.94103300
C	2.07216400	-1.49466300	-0.11760900
H	2.52634600	-2.47316300	-0.04506500
C	0.10023200	2.99285600	-1.48282300
C	0.22837100	2.31026800	-0.25740100
O	0.08795800	2.40671600	2.16047100
C	2.21869800	0.87354000	-0.11997100
H	2.77497500	1.80282500	-0.10326200
C	2.88287400	-0.35702000	-0.06896300
C	-0.38902100	4.35942300	0.90892400
H	-0.58355800	4.87128300	1.84503400
O	-4.94189700	-0.91296500	-0.04198600
C	4.35654800	-0.44991300	0.03675200
O	-2.12427700	-0.35476400	-3.28056100
C	-2.10036700	-0.33577600	-2.12488200
C	5.05503100	-1.50089000	-0.58339100
H	4.51543900	-2.23906500	-1.16864400
C	-0.27734400	4.33805300	-1.51662200
H	-0.36974500	4.83503800	-2.47615000
C	6.44310500	-1.58461600	-0.48518300
H	6.96847600	-2.39634500	-0.97898500
O	-3.02823700	2.48897800	-0.21037900
C	-2.37208300	-3.34923700	-0.31563600
H	-3.42648300	-3.10863500	-0.34971300
C	-1.95788300	-4.67592500	-0.30150300
H	-2.69649100	-5.46871600	-0.32206800
C	0.30070400	-3.88090400	-0.24175600
H	1.36434400	-4.07623700	-0.22010800
C	-0.59211800	-4.94647200	-0.26518700
H	-0.22482500	-5.96698300	-0.25762600
C	-2.54668300	1.44107600	-0.25834600
N	-1.51537400	-2.31211800	-0.28916900
C	-0.50614800	5.01152400	-0.31854600
H	-0.79051000	6.05937700	-0.34254600
C	5.08402600	0.51259500	0.75884400
H	4.56171200	1.31772900	1.26612700
C	6.47139200	0.42273700	0.86067900
H	7.01731900	1.16781600	1.43127700

C	7.15528900	-0.62465700	0.23821500
H	8.23616500	-0.69218100	0.31616800
C	-3.81616100	-0.68500700	-0.16879500
H	-0.29692100	1.50426800	2.14103100

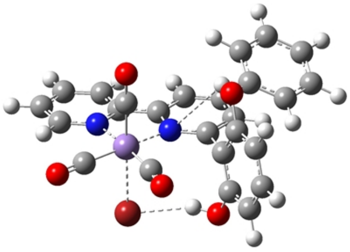

Optimized geometry of $[Mn(dhbpy)(CO)_3Br]^-$:

Br	2.19939200	-0.26290300	-2.27452200
Mn	2.01349800	-0.31109800	0.44843400
N	-0.04231200	-0.15780300	0.19089800
C	0.17329000	-2.55269400	0.16360200
O	-0.72251800	2.49011700	2.53708200
H	-1.08572100	1.61146700	2.34317600
C	-0.67833100	-1.40229500	0.12445900
C	-0.84964800	0.94299300	0.12978400
C	0.13930500	2.98130200	-1.01277200
C	-2.08274500	-1.50707800	0.03816200
H	-2.52653300	-2.49300200	-0.02424200
C	-0.31447400	3.06201000	1.36328300
C	-0.27425400	2.32491800	0.16405700
O	0.18135000	2.33973400	-2.21785300
C	-2.23105600	0.87008900	0.04565100
H	-2.79290200	1.79571900	0.02078900
C	-2.90151600	-0.39229000	0.00327500
C	0.48678300	4.33618200	-0.98666800
H	0.79831000	4.81319900	-1.90993300
O	4.91919400	-0.88754200	0.47950900
C	-4.37118600	-0.49241900	-0.09097100
O	1.72135400	-0.36476900	3.37094900
C	1.85306000	-0.33312700	2.21883500
C	-5.06590400	-1.60165400	0.43481600
H	-4.51638100	-2.38383300	0.94983800
C	0.05589700	4.40946200	1.40025300
H	0.01446100	4.94458000	2.34304300
C	-6.45244600	-1.69679900	0.33562900
H	-6.96123200	-2.56005500	0.75569500
O	2.98513300	2.49442000	0.44044500
C	2.37319400	-3.34033900	0.39376400
H	3.41986600	-3.09281700	0.52775500
C	1.98547500	-4.66400000	0.30364500
H	2.72703800	-5.45212300	0.36391800
C	-0.28068000	-3.89662800	0.06431100
H	-1.33616100	-4.10085100	-0.06891400
C	0.61050700	-4.94316100	0.13016400
H	0.25869000	-5.96716600	0.04974300
C	2.49974600	1.44283200	0.42692900
N	1.51986100	-2.29552500	0.32069400
C	0.44365200	5.03767600	0.21780000
H	0.72116000	6.08782400	0.23692600
C	-5.13038600	0.52246300	-0.70896800
H	-4.62752400	1.38118700	-1.14277700

C	-6.51829700	0.42709900	-0.80494800
H	-7.07655900	1.22048900	-1.29428200
C	-7.18918600	-0.68271000	-0.28462200
H	-8.27029900	-0.75519700	-0.35728000
C	3.78012500	-0.66994000	0.47416300
H	0.55312300	1.43590100	-2.12003300

Optimized geometry of the hydride anion $[Mn(dhbpy)(CO)_3H]^-$ obtained by migration of H from the ligand dhbpy to Mn.

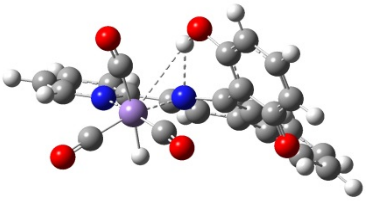

Mn	2.18718500	-0.33939700	-0.64637500
N	0.19710900	-0.14555500	0.23189600
C	0.53710600	-2.51688900	0.37448500
O	1.34971800	1.51122600	2.27757100
H	1.15681800	0.66685800	1.83651600
C	-0.39164700	-1.37688600	0.27877300
C	-0.61181800	0.95634900	0.23557000
C	-0.59654900	3.41843300	-0.31961800
C	-1.76370700	-1.56190200	0.18737100
H	-2.17250800	-2.56372100	0.15132100
C	0.89052900	2.52759200	1.47505300
C	-0.05546900	2.29520300	0.44672200
O	-1.45942000	3.26441800	-1.24358200
C	-2.00847600	0.80969400	0.11150600
H	-2.59743100	1.71459400	0.07764000
C	-2.60971500	-0.44364900	0.06372500
C	-0.08102300	4.71837900	0.02910000
H	-0.46368500	5.56690000	-0.53291900
O	4.29817300	-1.20559700	-2.49542900
C	-4.07762400	-0.59180000	-0.08688300
O	4.18142400	0.23768500	1.48733300
C	3.32550800	0.03318800	0.72718400
C	-4.76791000	-1.65629700	0.51853500
H	-4.22730800	-2.37200200	1.13049800
C	1.34929300	3.80869100	1.77795200
H	2.05913900	3.94317300	2.58725600
C	-6.14850000	-1.78707900	0.36865800
H	-6.66567000	-2.61119500	0.85123000
O	2.29302800	2.30528800	-1.96461800
C	2.72295400	-3.24649100	0.09288800
H	3.73474100	-2.99337800	-0.20094500
C	2.40727800	-4.52984700	0.52130700
H	3.18131100	-5.28757200	0.56442000
C	0.15023700	-3.78535600	0.82666200
H	-0.87207200	-3.96166500	1.13786500
C	1.09164200	-4.80529300	0.89660800
H	0.80718200	-5.79171200	1.24760000
C	2.23097800	1.30043900	-1.38595500
N	1.81535400	-2.25455400	0.01266100
C	0.84826900	4.89316900	1.03753400

H	1.20324300	5.89595900	1.27069200
C	-4.81019900	0.33685000	-0.84783400
H	-4.29037200	1.15266200	-1.34109100
C	-6.18970100	0.20322600	-0.99938900
H	-6.73706900	0.92526400	-1.59818800
C	-6.86443100	-0.85885800	-0.39133900
H	-7.93906900	-0.96207500	-0.50887500
C	3.49408900	-0.84483400	-1.73474500
H	1.32582700	-0.71675800	-1.93894800

Optimized geometry of the hydride dianion[Mn(dhbpy)(CO)$_3$H]$^{2-}$.

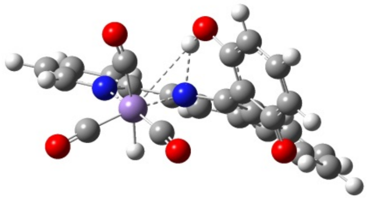

Mn	-2.17909200	-0.35945700	0.66290200
N	-0.21563200	-0.12820500	-0.21424700
C	-0.48987000	-2.51056000	-0.37743700
O	-1.24999100	1.43278800	-2.28568200
H	-1.03935500	0.62289600	-1.77507900
C	0.39424800	-1.38699500	-0.28797900
C	0.61354600	0.97415800	-0.19732500
C	0.47917900	3.46850400	0.35047800
C	1.79325000	-1.53418900	-0.21663600
H	2.20945200	-2.53502300	-0.18407300
C	-0.87011800	2.49462100	-1.49722900
C	0.02603700	2.31550200	-0.42134800
O	1.30375900	3.37929400	1.32120500
C	1.99358500	0.84881000	-0.10311300
H	2.57794800	1.75789600	-0.09452000
C	2.62565400	-0.43009800	-0.08215400
C	-0.07231300	4.73997200	-0.05153600
H	0.24649200	5.61319100	0.51436300
O	-4.33507200	-1.30194700	2.41920800
C	4.08616000	-0.56231100	0.07781100
O	-4.13505800	0.30788500	-1.47527000
C	-3.28456800	0.07557700	-0.71182700
C	4.79451000	-1.67404600	-0.42759300
H	4.26073000	-2.44338800	-0.97771200
C	-1.37230200	3.75094100	-1.85401300
H	-2.05024900	3.83691600	-2.69740300
C	6.17281500	-1.79050000	-0.26176200
H	6.68949200	-2.65637700	-0.66749800
O	-2.28304900	2.22774300	2.08199100
C	-2.70532600	-3.26238500	-0.18815300
H	-3.73318800	-3.00604500	0.05106600
C	-2.37676200	-4.55587000	-0.56472900
H	-3.14521600	-5.31778900	-0.62894300
C	-0.09417000	-3.81813300	-0.77391000
H	0.94154000	-4.00496200	-1.03570100
C	-1.02150900	-4.83303500	-0.86186500
H	-0.71623800	-5.82751200	-1.17473500
C	-2.21926900	1.24106500	1.46560400
N	-1.81461900	-2.26041000	-0.07638400

C	-0.95533600	4.86598200	-1.11176200
H	-1.33600600	5.85149900	-1.37914000
C	4.83186200	0.43319100	0.74624400
H	4.31579400	1.29156100	1.16542900
C	6.21188800	0.31710000	0.90837500
H	6.75613000	1.09657000	1.43532200
C	6.89414200	-0.79509200	0.40704000
H	7.96943400	-0.88407300	0.53138100
C	-3.50989000	-0.91031000	1.69102100
H	-1.33506700	-0.82613600	1.95027400

References

[1] Ciupa, A; Mahon, M. F.; De Bank, P. A.; Caggiano, L.; *Org. Biomol. Chem.*, **2012**, 10, 8753–8757

[2] Basnet, A; Thapa, P; Karki, R; Na, Y;Jahng, Y; Jeong, B.S; Jeong, T.C; Leec, C.S;Leea, E.S; *Bioorg. Med. Chem.*, **2007**, 15, 4351–4359

[3] Neve, F; Ghedini, M; Francescangeli, O; Campagna, S.; *Liquid Crystals*, **1998**, 24, 5, 673-680

[4] Laye, R. H.;Couchman, S. M.; Ward, M. D.; *Inorg. Chem.* 2001, 40, 4089-4092

[5] Agilent Technologies UK Ltd., Oxford, U.K

[6] Agilent Technologies (20129. CrysAlisPro Software system, version 1.171.35.11, Agilent Technologies U. K. Ltd., Oxford, U.K..

[7] G.M. Sheldrick, SHELXTL, (1997), Göttingen, Germany

[8] a) C.Costentin, M. Robert and J. M.Saveant, *Chem. Soc. Rev*, 2013, **42**, 2423; b) C.Costentin, S.Drouet, M. Robert, and J. M.Savéant, *J. Am. Chem. Soc,* 2012, **134**, 11235−11242; c) J. M. Saveant, *Chem. Rev.*, 2008, **108**, 2348

[9] a) J. M. Smieja, M. D. Sampson, K. A. Grice, E. E. Benson, J. D. Froehlich,C. P. Kubiak, *Inorg. Chem.*, 2013, ***52***, 2484 ; b) M. D. Sampson, A. D. Nguyen, K. A. Grice, C. E. Moore, A. L. Rheingold and C. P. Kubiak, *J. Am. Chem. Soc.*, 2014, ***136***, 5460

[10] C. Costentin, S. Drouet, M. Robert, J. M.Saveant, *Science* 2012, **338**, 90